JACS
JOURNAL OF THE AMERICAN CHEMICAL SOCIETY
Article
pubs.acs.org/JACS

An Endohedral Metallofullerene as a Pure Electron Donor: Intramolecular Electron Transfer in Donor–Acceptor Conjugates of $La_2@C_{80}$ and 11,11,12,12-Tetracyano-9,10-anthra-*p*-quinodimethane (TCAQ)

Yuta Takano,[†] Shota Obuchi,[†] Naomi Mizorogi,[†] Raúl García,[‡] M. Ángeles Herranz,[‡] Marc Rudolf,[§] Dirk M. Guldi,*[,§] Nazario Martín,*[,‡,∥] Shigeru Nagase,*[,⊥] and Takeshi Akasaka*[,†]

[†]Life Science Center of Tsukuba Advanced Research Alliance, University of Tsukuba, Tsukuba, Ibaraki 305-8577, Japan

[‡]Departamento de Química Orgánica I, Facultad de Química, Universidad Complutense, E-28040 Madrid, Spain

[§]Department of Chemistry and Pharmacy and Interdisciplinary Center for Molecular Materials (ICMM), Friedrich-Alexander-Universität Erlangen-Nürnberg, Egerlandstrasse 3, 91058 Erlangen, Germany

[∥] IMDEA - Nanoscience, Campus de Cantoblanco, E-28049 Madrid, Spain

[⊥] Fukui Institute for Fundamental Chemistry, Kyoto University, Kyoto, Kyoto 606-8103, Japan

Supporting Information

ABSTRACT: An endohedral metallofullerene, $La_2@C_{80}$, is covalently linked to the strong electron acceptor 11,11,12,12-tetracyano-9,10-anthra-*p*-quinodimethane (TCAQ) by means of the Prato reaction, affording two different [5,6]-metallofulleropyrrolidines, namely **1a** and **2a**. **1a** and **2a** were isolated and fully characterized by means of MALDI-TOF mass, UV–vis–NIR absorption, and NMR spectroscopies. In addition, cyclic voltammetry (CV) and differential pulse voltammetry (DPV) corroborated the unique redox character of **2a**, that is, the presence of the electron-donating $La_2@C_{80}$ and the electron-accepting TCAQ. Although a weak electronic coupling dictates the interactions between $La_2@C_{80}$ and TCAQ in the ground state, time-resolved transient absorption experiments reveal that in the excited state (i.e., π–π^* centered at $La_2@C_{80}$) the unprecedented formation of the $(La_2@C_{80})^{\bullet+}$–$(TCAQ)^{\bullet-}$ radical ion pair state evolves in nonpolar and polar media with a quantum efficiency of 33%.

INTRODUCTION

Organic photovoltaic cells are currently attracting much attention as a means to convert semipermanent solar energy into renewable energy sources.[1] A full plethora of multicomponent electron donor–acceptor conjugates and hybrids have been devised in recent years, whose studies of photoinduced processes (including energy and electron transfer) have advanced our understanding of artificial photosynthetic and photovoltaic systems.[2,3]

In this regard, concerted efforts toward the development of electron donor–acceptor conjugates and hybrids have documented the physicochemical assets of fullerenes as symmetrical three-dimensional structures. In particular, fullerenes accept multiple electrons in solution at moderate potentials to form stable monoanionic, dianionic, etc. species. Most importantly, fullerenes and their derivatives exhibit low reorganization energies in electron transfer reactions, which render them promising for energy conversion and energy storage devices.[2,4] As a matter of fact, over 7% energy photocurrent efficiency (PCE) has been reported for fullerene derivatives as an integrative component in bulk heterojunction solar cells.[5]

Among the different classes of fullerenes, *endohedral metallofullerenes*, which encapsulate one or more metal atoms in their interior, are unique owing to the fact that their physicochemical properties (including ground and excited state features) depend in large part on the nature and the composition of the encapsulated species.[6] A remarkable demonstration of the potential of endohedral metallofullerenes has been their application in the field of organic solar cells. The use of 1-(3-hexoxycarbonyl)propyl-1-phenyl-[6,6]–$Lu_3N@C_{81}$ ($Lu_3N@C_{80}$–PCBH) and poly(3-hexylthiophene) P3HT has led to significantly larger open circuit voltages (0.89 V vs 0.63 V) and appreciably higher PCEs (4.2% vs 3.4%) than in C_{60}-PCBM/P3HT reference devices under AM1.5 solar simulation conditions.[7] Furthermore, among the organic conductors that were probed by flash-photolysis time-resolved microwave conductivity, a single-crystal of an adamantylidene derivative of $La@C_{82}$ exhibited the highest ever reported electron mobility (μ) exceeding 10 $cm^2\ V^{-1}\ s^{-1}$.[8] Such remarkable chemical and physical features have inspired chemists to design

Received: July 26, 2012
Published: November 2, 2012

 © 2012 American Chemical Society dx.doi.org/10.1021/ja307341g | J. Am. Chem. Soc. 2012, 134, 19401–19408

and synthesize novel derivatives of endohedral metallofullerenes as building blocks for optoelectronic materials.

Recently, we have demonstrated that, in contrast to the photoreactivity of C_{60}–perylenebisimide (C_{60}–PDI), in which a cascade of energy transfer processes evolve, PDI acts in $Lu_3N@C_{80}$–PDI as the light harvester and the electron acceptor. In particular, photoexcitation of $Lu_3N@C_{80}$–PDI triggers a photoinduced electron transfer from the ground state of $Lu_3N@C_{80}$ to the singlet excited state of PDI.[9] Notably, $La_2@C_{80}$ and trimetallic nitride template endohedral metallofullerenes (including $Lu_3N@C_{80}$) reveal marked differences in terms of their redox potentials as well as their molecular orbitals.[10] Although $La_2@C_{80}$ and $Lu_3N@C_{80}$ feature similar oxidation potentials (+0.56 V vs +0.64 V against $Fc^{0/+}$), $La_2@C_{80}$ gives rise to a much lower first reduction potential (−0.31 V) compared to that of $Lu_3N@C_{80}$ (−1.40 V)[11]and, which is important in the context of the current work, even lower than the one of PDI (−0.89 V).[9] Whereas the LUMOs, as a reflection of the reduction potentials, are localized on the encapsulated metal atoms in the case of $La_2@C_{80}$, those of $M_3N@C_{80}$ (M = Sc, Y and Lu) are delocalized over the trimetallic nitride template and the fullerene. As a matter of fact, the remarkable redox features of $La_2@C_{80}$ are likely to impact key aspects in photoinduced intramolecular electron transfer reactions such as pathways, dynamics, and quantum yields.

Another recent report documents that an endohedral metallofullerene, namely $Ce_2@C_{80}$, functions as a stable electron donor that transfers an electron to photoexcited zinc porphyrins.[12] In fact, a systematic investigation of the electron transfer chemistry reveals the formation of the radical ion pair $(Ce_2@C_{80})^{\bullet-}$–$(ZnP)^{\bullet+}$ in nonpolar media (i.e., toluene and THF), while the formation of $(Ce_2@C_{80})^{\bullet+}$–$(ZnP)^{\bullet-}$ species dominates in polar media (i.e., benzonitrile and DMF). Notably, such a switching electron donor/acceptor behavior is a unique phenomenon for $Ce_2@C_{80}$ and $La_2@C_{80}$, which is absent in all empty fullerenes and in most endohedral metallofullerenes. The rather poor electron acceptor strength of zinc porphyrins evokes, nevertheless, the solvent dependent electron transfer mechanism.

Solvent independent electron transfer is, however, a desirable feature to realize the versatile use of endohedral fullerenes as electron donors, especially considering the nonpolar environment in organic solar cells. In addition, although various electron donor–acceptor conjugates of C_{60} have been well-studied, only one example, to the best of our knowledge, is available for the electron transfer system, in which a fullerene acts as an electron donor.[13] However, the presence of $Sc(OTf)_3$ as an oxidation reagent is needed in the example. Tetracyanoanthra-*p*-quinodimethanes (TCAQ) stand out among electron acceptors and, as such, they play a crucial role in electron transfer reactions, molecular rectifiers, transport layers in organic optoelectronic devices, and electrochiroptical materials.[14] Moreover, highly distorted TCAQs undergo aromatization upon reduction, which causes a dramatic geometrical change and results in the formation of thermodynamically stable dianionic species at relatively low reduction potentials.[15] In light of the aforementioned, we have designed, synthesized, and probed a novel electron donor–acceptor conjugate, in which the strong electron-accepting TCAQ is linked to $La_2@C_{80}$.

Scheme 1

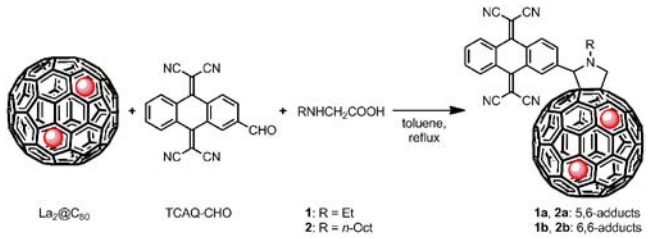

RESULTS AND DISCUSSION

Synthesis and Structural Determination. The target metallofulleropyrrolidines were synthesized using the synthetic procedures of 1,3-dipolar cycloaddition reactions, in which reactive azomethine ylides generated from aminoacetic acids and aldehydes react with $La_2@C_{80}$, the so-called Prato reaction (Scheme 1).[16] A close look at the HPLC elugrams of the reaction mixtures suggest the formation of major products **1a** and **2a**, respectively (Figure 1). The results attest that the

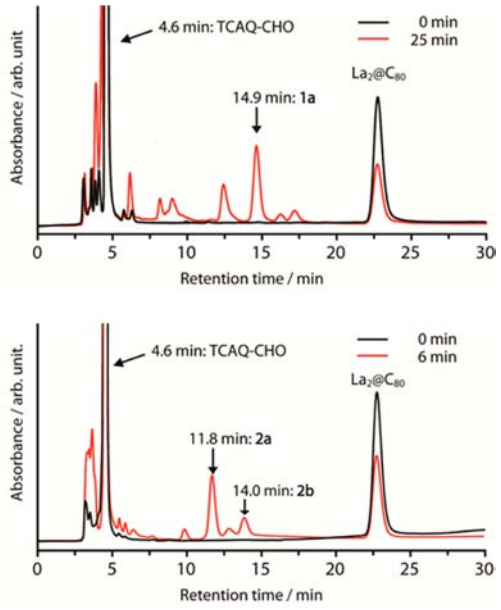

Figure 1. HPLC profiles of the reaction crudes of **1** (top) and **2** (bottom). Conditions: 5PYE column (i.d. 4.6 mm × 250 mm); toluene eluent; 1.0 mL/min flow rate; 330 nm wavelength; 40 °C temperature.

reaction using TCAQ-CHO proceeds more than 5 times faster than those of Ph-CHO or 2-formyl-9,10-bis(1,3-dithiol-2-ylidene)-9,10-dihydroanthracene (exTTF-CHO).[17] Here, the electron-withdrawing effect of TCAQ increases the reactivity of the azomethine ylide.[18]

1a and **2a** were isolated from byproducts and unreacted materials in a one-step HPLC separation using a Buckyprep column. The purities of **1a** and **2a** are greater than 98% using HPLC analyses with various columns see Figure 2 and Supporting Information (SI). Interestingly, the retention times of **2a** in the HPLC profiles are shorter than those of **1a**, which suggests that the *n*-octyl chains suppress intermolecular interactions between **2a** and the HPLC columns and that accelerates the elution of **2a**.

The MALDI-TOF mass spectra of **1a** and **2a** show molecular ion peaks at 1611 and 1695 *m*/*z*, respectively (Figure 3). As

dx.doi.org/10.1021/ja307341g | J. Am. Chem. Soc. 2012, 134, 19401–19408

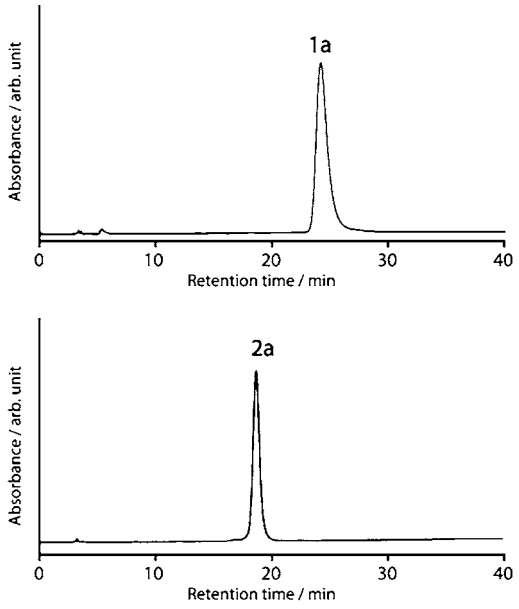

Figure 2. HPLC profiles of isolated **1a** (top) and **2a** (bottom). Conditions: Buckyprep column (i.d. 4.6 mm × 250 mm) ; toluene eluent; 1.0 mL/min flow rate; 330 nm wavelength; 40 °C temperature.

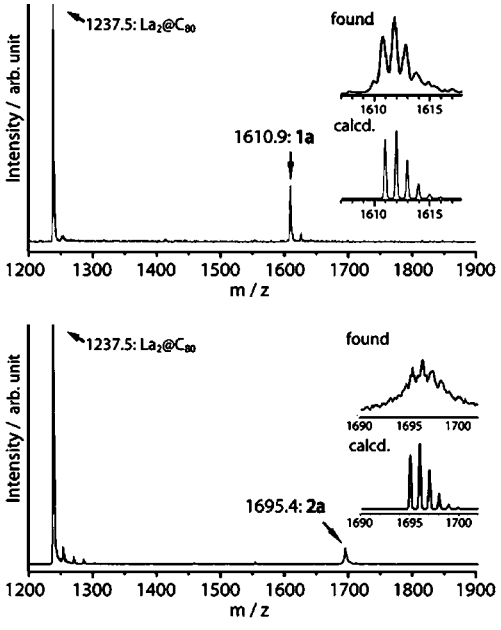

Figure 3. MALDI-TOF mass spectra of isolated **1a** (top) and **2a** (bottom). Conditions: negative mode, matrix; 1,1,4,4-tetrapheny-1,3-butadiene.

such, the molecular ion peaks confirmed the isolation of the target metallofulleropyrrolidines consisting of $La_2@C_{80}$ and TCAQ. The major fragment peak at 1238 m/z correlates with pristine $La_2@C_{80}$ generated during laser desorption.

The UV−vis−NIR spectra of **1a** and **2a** resemble each other and those Prato adducts of [5,6]-closed nature $La_2@C_{80}(CH_2)_2NTrt$ (**3a**),[19] but clearly differ from the [6,6]-closed analogue of $La_2@C_{80}(CH_2)_2NTrt$ (**3b**)[19] (Figure 4). In particular, the spectral similarities, especially in the vis−NIR region, imply isostructural characteristics due to the same [5,6]-closed addition pattern. In general, the absorption spectra of fullerene derivatives provide distinct fingerprints in the vis−

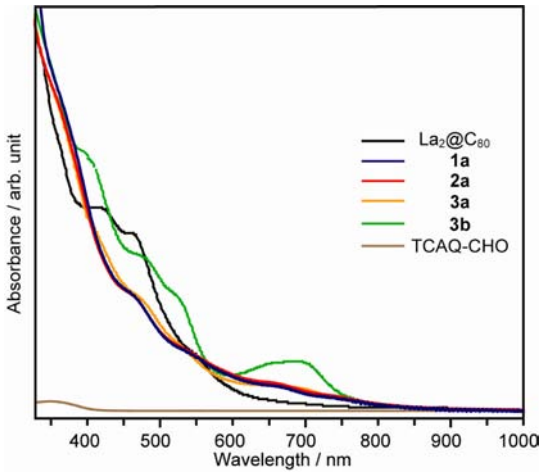

Figure 4. UV−vis−NIR absorption spectra of $La_2@C_{80}$, TCAQ-CHO, **1a**, **2a**, **3a**,[19] and **3b**[19] in toluene.

NIR region that relate to the nature of the π-electron system. Thus, it is safe to conclude that **1a**, **2a**, and **3a** all have the same [5,6]-closed addition pattern.

Further characterization of **1a** and **2a** was based on ^{1}H NMR measurements.[20] The ^{1}H NMR spectrum of **2a** gives rise to signals that correspond to the pyrrolidine protons between δ 3.1 and 4.5 (Figure 5). The resonances due to the aromatic

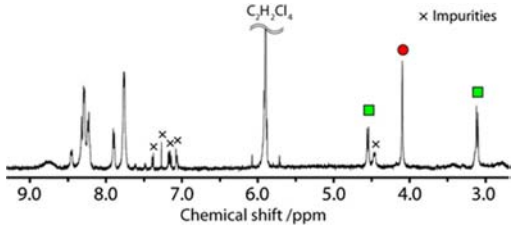

Figure 5. ^{1}H NMR spectra of **2a** between 3 and 9 ppm at 500 MHz in 1:3 (v/v) $C_2D_2Cl_4/CS_2$ at 293 K. Signals marked by green squares and red circles are attributed respectively to the pyrrolidine geminal and methyne protons.

protons of the anthracenyl group in TCAQ evolve around δ 7.7−8.8. For **1a**, all of the aforementioned ^{1}H NMR signals appear in the same magnetic field regions with the exception of those that relate to the alkyl chains (Figure S3, SI). Finally, the chemical shifts seen for the geminal protons in **1a** and **2a** are in good agreement with the values reported for the [5,6]-closed metallofulleropyrrolidine **3a** and differ distinctly from those of the [6,6]-closed analogue **3b**,[17,19] which further corroborates the [5,6]-closed addition pattern of **1a** and **2a** initially proposed on the basis of the absorption spectra (vide supra).

Complementary DFT calculations suggest that the most feasible structure of **1a** is the [5,6]-isomer I, in which TCAQ adopts a *cis* conformation relative to the two dicyanovinylenes (Figure 6). The *cis* conformation is thermodynamically more stable than that of the *trans* conformation by 10.7 kcal/mol (Figure S4, SI). Notably, this finding is consistent with a previous report on C_{60}-TCAQ.[21] The computational results also suggest that the *cis*1-[5,6]-isomer I is in the lowest energy configuration among the eight possible [5,6]-isomers (+1.4 to +10.4 kcal/mol) (Figure S5, SI). In comparison with [5,6]-isomers, [6,6]-isomers are 2.50 kcal/mol less stable (Figure S6, SI). The latter is in good agreement with the experimental

dx.doi.org/10.1021/ja307341g | J. Am. Chem. Soc. 2012, 134, 19401−19408

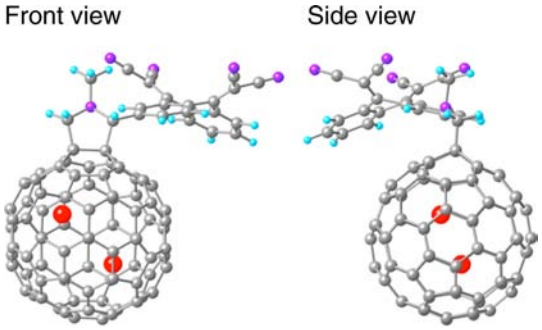

Figure 6. Most stable optimized structure of **1a** (in which ethyl group is substituted to methyl group for simplification) calculated at the M06-2X/6-31G(d)[C, H, N], LanL2DZ[La] level of theory.

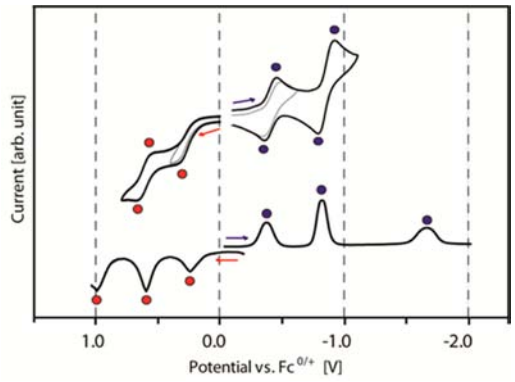

Figure 7. CV (upper) and DPV (lower) of **2a** measured in *o*-dichlorobenzene at room temperature.

Table 1. Redox Potentials[a,b]

cmpd	$E_{ox}^{(3)}$	$E_{ox}^{(2)}$	$E_{ox}^{(1)}$	$E_{red}^{(1)}$	$E_{red}^{(2)}$	$E_{red}^{(3)}$
2a	0.98[c]	0.59	0.24[c]	−0.45	−0.91	−1.66[c]
TCAQ-CHO				−0.72		
4[d]	1.00[c]	0.59	0.20	−0.44	−1.70	−2.22[c]
$La_2@C_{80}$[e]		0.95[c]	0.56	−0.31	−1.71	−2.13[c]

[a]Values are given in volts relative to a $Fc^{0/+}$ redox couple and were obtained from DPVs. [b]Conditions: working electrode and counter electrode, platinum wires; reference electrode, SCE; supporting electrolyte, 0.1 M $TBAPF_6$ in *o*-DCB. CV: scan rate, 50 mV s^{-1}. DPV: pulse amplitude, 50 mV; scan rate, 20 mV s^{-1}. [c]Irreversible. [d]Data from ref 15. [e]Data from ref 10.

results summarized before and those that will be discussed in the following paragraph about the second major products (vide infra).

The second major product of **2** was partially identified. **2b** was purified using preparative HPLC (Figure S7, SI) and was subjected to MALDI-TOF mass spectrometry characterization (Figure S8, SI). The spectrum of **2b** portrays the molecular ion peak at 1695 *m*/*z*, which is the same mass number of **2a**, suggesting that **2b** is a site-isomer of **2a**. Notably, "site-isomer" refers in this context to an isomer of the adduct with the same fullerene and the same addend but a different addition position—a classification proposed recently by Martín et al.[22] Such a notion is further supported by the absorption spectrum of **2b**. The latter resembles that of the [6,6]-adduct **3b**[19] (Figure S9, SI). It is well-known that [5,6]-adducts of endohedral metallofullerenes of C_{80} are the thermodynamically favored products, while the kinetically preferred products are the [6,6]-adducts.[23] Our theoretical calculations, as shown in Figure S6 (SI), confirm this trend. The reaction with TCAQ-CHO affords the kinetically favored [6,6]-isomer **2b** as the second major product.

Electronic properties. Figure 4 documents that the absorption spectra of **1a** and **2a** give rise to the absorptions of [5,6]-closed fulleropyrrolidines of $La_2@C_{80}$ and TCAQ. Neither for **1a**, nor for **2a** we gathered any appreciable spectroscopic evidence for a charge transfer in the ground state. These results suggest that only weak, if any, intramolecular electron interactions prevail between $La_2@C_{80}$ and TCAQ in the ground state. In addition, the nature of the $La_2@C_{80}$-centered absorptions in **1a** and **2a** is ascribed to $\pi-\pi^*$ transitions. On one hand, the energetic mismatch of the long wavelength absorption onset/short wavelength emission (1.4 ± 0.2 eV) relative to charge transfer interactions involving the La cluster (1.04 eV) should be considered. On the other hand, the bathochromic shift of the absorptions when probing polar solvents is another important criterion.

Electrochemical properties of **2a** were determined by means of cyclic voltammetry (CV) and differential pulse voltammetry (DPV) (Figure 7 and Table 1). The first reduction is associated with the one-electron reduction of the La cluster in $La_2@C_{80}$. In stark contrast, the second reduction is a two-electron reduction step and involves TCAQ.[14,15] All of the oxidations, as they are listed in Table 1, are attributed to one-electron oxidations of $La_2@C_{80}$. This assignment finds further support by theoretical calculations, which implies that HOMO and HOMO−1 are localized on $La_2@C_{80}$ (Figure S10, SI). In addition, pyrrolidine adducts of fullerenes are known to show a reversible or a quasi-reversible oxidation step, depending on the fullerene structure and connecting moieties.[24] As such, all of the $La_2@C_{80}$ centered reduction and oxidation processes are identical with those of $La_2@C_{80}CH_2NEtCHPh$ (**4**),[17] which is a metallofulleropyrrolidine that is based on $La_2@C_{80}$ and that lacks TCAQ. Taking the aforementioned into concert, we reach the important conclusion that the introduction of TCAQ does not influence the redox properties of $La_2@C_{80}$ in the ground state—a result that agrees well with the absorption assays. Using the potentials corresponding to the first one-electron oxidation of $La_2@C_{80}$ (+0.24 V) and to the first one-electron reduction of TCAQ (−0.91 V), the energy of the $(La_2@C_{80})^{\bullet+}-(TCAQ)^{\bullet-}$ radical ion pair state was determined as 1.15 eV.

In femtosecond transient absorption measurements with **2a** (Figure 8), immediately after the laser excitation, strong singlet−singlet absorptions with maxima at 515, 575, 910, and 1100 nm and a minimum at 465 nm are discernible. Important is the similar intensity of the 910 and 1100 nm maxima. These features resemble those seen for $La_2@C_{80}CH_2NEtCHPh$ **4** (Figure S11, SI) and thus confirm that, despite the presence of TCAQ, the $La_2@C_{80}$ singlet excited state is formed. When compared to **4** (33 ± 5 ps), the singlet−singlet absorptions decay in **2a** with accelerated dynamics in, for example, THF (10 ± 5 ps). Spectroscopically, the transient absorption changes, which occurred after the completion of the decay, bear no resemblance to that of the $La_2@C_{80}$ triplet excited state—compare Figure 8 and Figure S12 (SI).[17] In the visible region, the sharp negative and positive absorptions at 465 and 570 nm, respectively, correspond to the one-electron reduced form of TCAQ.[25] In the near-infrared region, the maxima between 800 and 1200 nm agree with the spectroelectrochemical signatures of the one-electron oxidized

dx.doi.org/10.1021/ja307341g | J. Am. Chem. Soc. 2012, 134, 19401−19408

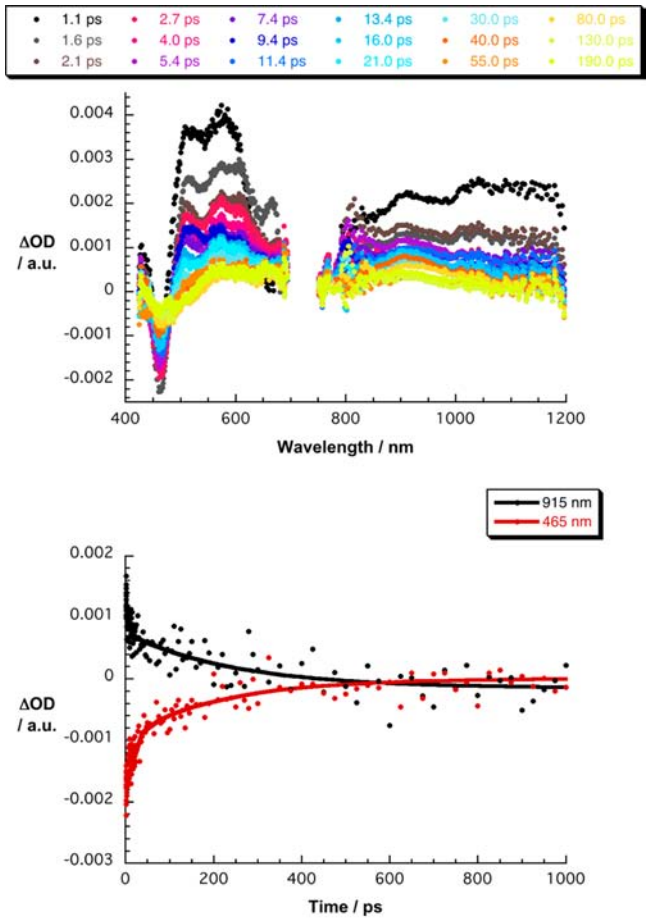

Figure 8. (Top) Differential absorption changes (ΔOD) in the visible and near-infrared region obtained upon femtosecond flash photolysis (387 nm) of **2a** (~10^{-5} M) in argon-saturated THF with several time delays between 0 and 200 ps at room temperature (see legend for details related to time progression). (Bottom) Time vs differential absorption changes (ΔOD) of the spectra shown above in THF at 465 and 915 nm, monitoring charge separation and charge recombination.

$La_2@C_{80}$ in **4** and relates to the one-electron oxidation of C_{80} in $La_2@C_{80}$. The latter feature a characteristic maximum at 905 nm followed by a much weaker transient around 1100 nm (Figure 9). Please note that despite the spectral similarity with the singlet excited state (vide supra) the intensity ratio of the 905 and 1100 nm maxima is decisive for our assignment. In other words, the close spectral resemblance between spectroelectrochemistry and photochemistry prompts for **2a** in THF to the unprecedented formation of the $(La_2@C_{80})^{\bullet+}$–$(TCAQ)^{\bullet-}$ radical ion pair state with a quantum efficiency of ~33% from the singlet excited state precursor (1.4 ± 0.2 eV) determined in absorption/fluorescence experiments. The time–absorption profiles show that this highly exergonic state is metastable. In fact, multiwavelength analyses provide lifetimes of 230 ± 15 ps in THF (Figure 8). In less polar solvents, namely cyclohexanecarbonitrile, toluene, and carbon disulfide, the corresponding radical ion pair state lifetimes are 80 ± 30, 110 ± 10, and 130 ± 15 ps, respectively see Figure 10. It is, however, the triplet excited state (1.0 ± 0.1 eV) of the $La_2@C_{80}$ moiety, whose energy was determined in phosphorescence experiments, that is formed in all of the tested solvents as the stable product of charge recombination. Support for this assumption came from complementary nanosecond experiments (Figure S12, SI) in which a long-lived transient is seen for **2a** in agreement with the reference experiments performed

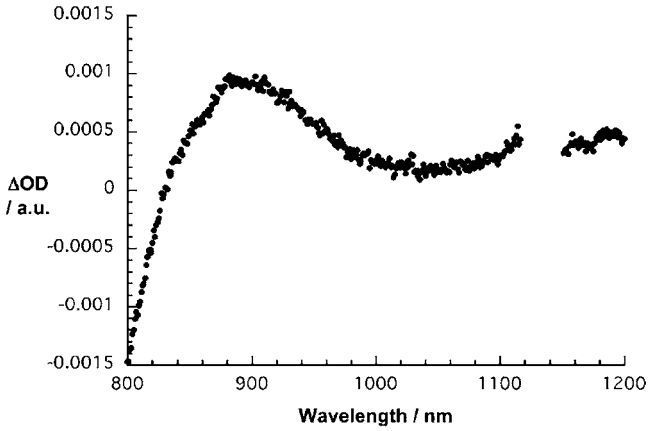

Figure 9. Differential absorption changes (ΔOD) in the near-infrared region obtained upon electrochemical oxidation of $La_2@C_{80}CH_2NEtCHPh$ (**4**) at an applied bias of +0.4 V in argon-saturated *o*-dichlorobenzene with 0.05 M $(n\text{-Bu})_4NPF_6$ as supporting electrolyte at room temperature.

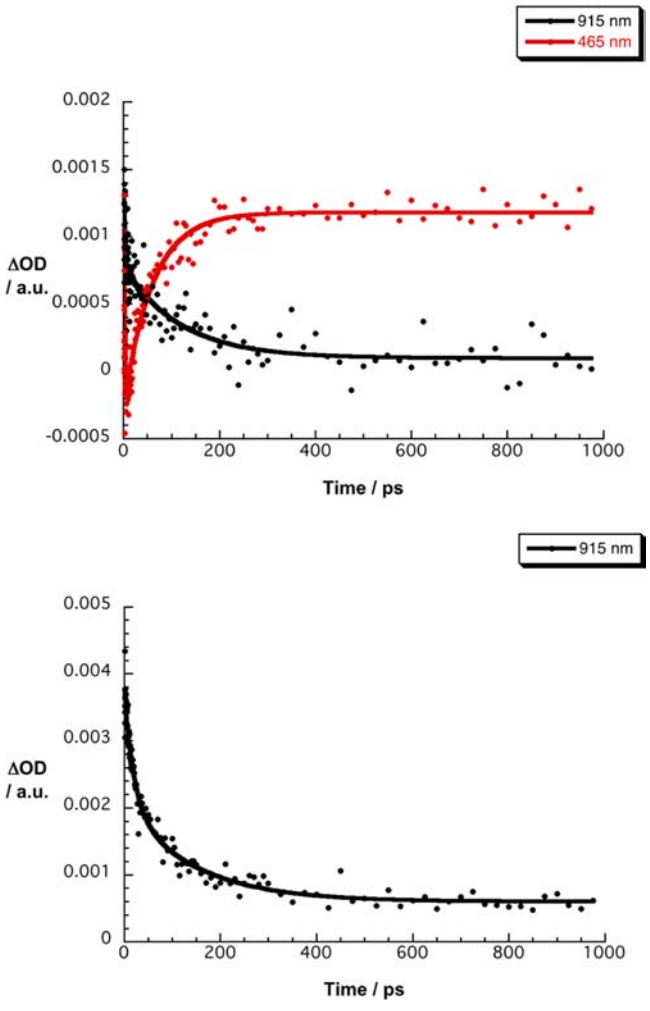

Figure 10. (Top) Time vs differential absorption changes (ΔOD) of **2a** in toluene at 465 and 915 nm, monitoring charge separation and charge recombination. (Bottom) Time vs differential absorption changes (ΔOD) of **2a** in carbon disulfide at 915 nm, monitoring charge separation and charge recombination.

dx.doi.org/10.1021/ja307341g | J. Am. Chem. Soc. 2012, 134, 19401–19408

with pristine $La_2@C_{80}$ and **4**.[17] In line with the phosphorescence experiments, the triplet excited state lifetime differs between the absence and the presence of molecular oxygen 29.6 ± 1.0 vs 27.5 ± 1.0, respectively. In fact, the molecular oxygen quenching of the triplet excited state goes hand in hand with the detection of singlet oxygen emission at 1275 nm and, as such, confirms the triplet excited state energy of **4**.

CONCLUSION

In summary, we have synthesized, characterized, and probed two novel metallofulleropyrrolidines (**1a** and **2a**) bearing the strong electron acceptor, TCAQ. Our results in terms of ground state characterization point to the lack of significant electronic interactions between TCAQ and $La_2@C_{80}$. However, in the excited state the reactivity differs fundamentally see Figure 11. Here, $La_2@C_{80}$, once photoexcited, acts in its singlet

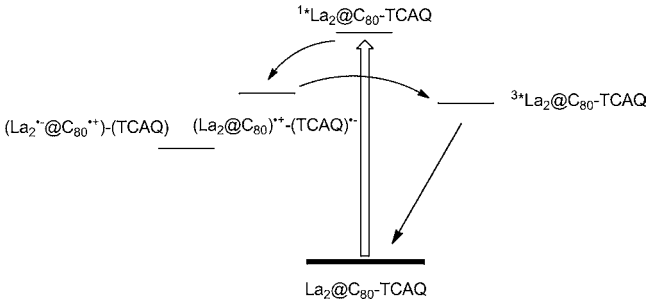

Figure 11. Energy diagram for **2a** illustrating the deactivation processes upon photoexcitation of $La_2@C_{80}$.

excited state (1.4 ± 0.2 eV) as an electron donor to yield a spatially separated radical ion pair state (1.15 eV) with a lifetime of several hundred picoseconds and featuring a one-electron reduced TCAQ and a one-electron oxidized $La_2@C_{80}$ before populating the triplet excited state (1.0 ± 0.1 eV) and, subsequently, the ground state in the absence of molecular oxygen. On one hand, the unique electron acceptor character of TCAQ and, on the other hand, the strong electron donor character of $La_2@C_{80}$ are of greatest importance to afford *for the first time* a radical ion pair state in nonpolar as well as polar media. Despite the simplicity, **1a** and **2a** show their potential for electron transport in molecular systems. However, the lack of a stable, isolable, empty fullerene C_{80} (due to the violation of the isolated pentagon rule) unfortunately hinders a meaningful comparison between $La_2@C_{80}$ and C_{80}.

EXPERIMENTAL SECTION

General Methods. All chemicals and solvents were obtained from Wako Pure Chemical Inds. Ltd. and were used without further purification unless otherwise stated. *o*-Dichlorobenzene was distilled over calcium hydride at reduced pressure under an argon atmosphere before use in reactions. Analytical high-performance liquid chromatography (HPLC) was performed on a HPLC apparatus (Jasco Inc.) using 5PYE, Buckyprep, Buckyprep M, or 5PBB columns (4.6 mm × 250 mm; Nacalai Tesque Inc.) with monitoring of UV absorption at 330 nm. Toluene was used as the eluent. The ^{1}H measurements were conducted on a spectrometer (AVANCE 500; Bruker Analytik GmbH) with a CryoProbe system, where TMS was used as an internal reference (δ = 0.00 ppm). Absorption spectra were recorded using a spectrophotometer (UV-3150; Shimadzu Corp.). Mass spectrometry was conducted using a mass spectrometer (BIFLEX III; Bruker Analytik GmbH) with 1,1,4,4-tetraphenyl-1,3-butadiene as a matrix. Cyclic voltammograms (CVs) and differential pulse voltammograms (DPVs) were recorded using an electrochemical analyzer (ALS630D; BAS Inc.). Platinum wires were used as the working and counter electrodes. The reference electrode was a saturated calomel reference electrode (SCE) filled with 0.1 M (*n*-Bu)$_4$NPF$_6$ (TBAPF$_6$) in *o*-DCB. All potentials are referenced to the ferrocene/ferrocenium couple (Fc/Fc$^+$) as the standard. CVs were recorded using a scan rate of 50 mV/s, and DPVs were obtained using a pulse amplitude of 50 mV, a pulse width of 50 ms, a pulse period of 200 ms, and a scan rate of 20 mV/s. The solution was deaerated for 20 min with argon before electrochemical measurements. The spectroelectrochemical measurements were done on a Varian Cary 5000 UV−vis−NIR spectrophotometer connected to a Princeton PGstat 263A using a homemade cell with three-electrode configuration. A light-transparent platinum gauze, a platinum plate, and a silver wire were employed as the working, counter, and reference electrodes, respectively. Femtosecond transient absorption studies were performed with 387 nm laser pulses (1 kHz, 150 fs pulse width) from an amplified Ti:Sapphire laser system (Clark-MXR, Inc.), the laser energy was 200 nJ. Nanosecond laser flash photolysis experiments were performed with 355 nm laser pulses from a Quanta-Ray CDR Nd:YAG system (6 ns pulse width) in a front face excitation geometry.

Synthesis of 2-Formyl-11,11,12,12-tetracyano-9,10-anthra-p-quinodimethane (TCAQ-CHO). TCAQ-CHO was prepared according to previously reported synthetic procedures,[21] and were identified using the spectroscopic data thereof.

*General Procedure for the Synthesis of Metallofulleropyrrolidines **1** and **2**.* A toluene solution containing $La_2@I_h$−C_{80} was refluxed with 10 equiv of aminoacetic acid and the corresponding aldehyde under argon atmosphere. After a variable period of time, the reaction mixture was injected into a preparative Buckyprep column (20 mm × 250 mm i.d.; Cosmosil, Nacalai Tesque Inc.) to separate **1a**, **2a**, and **2b** from byproducts and unreacted starting materials.

*5,6-$La_2@C_{80}CH_2NEtCH$-TCAQ (TCAQ = $C_{20}H_7N_4$) (**1a**).* In 160 mL of toluene (4.0×10^{-4} M) was dissolved 8.00 mg of $La_2@I_h$-C_{80}. The mixture was then refluxed for 25 min after the addition of 12.1 mg of *N*-ethyl glycine and 21.5 mg of TCAQ-CHO. Yield: 42.4% (based on consumed starting fullerene). ^{1}H NMR (500 MHz, $CS_2/C_2D_2Cl_4$, 3/1, 293 K) δ: 8.70 (s, 1H), 8.30−8.28 (m, 2H), 8.25 (d, 1H, J = 7.3 Hz), 7.92 (d, 1H, J = 7.3 Hz), 7.76 (d, 2H, J = 7.0 Hz), 4.57 (d, 1H, J = 9.5 Hz), 4.12 (s, 1H), 3.55 (CH_2, 2H), 3.12 (d, 1H, J = 9.5 Hz), 1.40 (t, 3H, J = 6.5 Hz). MALDI-TOF MS calculated for $C_{104}H_{15}La_2N_5$ ([M]$^-$): 1610.95, found: 1610.51 m/z.

*5,6-$La_2@C_{80}CH_2NOctCH$-TCAQ (**2a**).* In 122 mL of *o*-DCB (4.0×10^{-4} M) was dissolved 6.10 mg of $La_2@I_h$-C_{80}; The mixture was then heated at 110 °C for 11 min after the addition of 9.23 mg of *N*-*n*-octylglycine and 16.4 mg of TCAQ-CHO. Yield: 50.2% (based on consumed starting fullerene). ^{1}H NMR (500 MHz, $CS_2/C_2D_2Cl_4$, 3/1, 293 K) δ: 8.76 (s, 1H), 8.32−8.28 (m, 2H), 8.23 (d, 1H, J = 8.0 Hz, 7.90 (d, 1H, J = 8.0 Hz), 7.76 (d, 2H, J = 6.5 Hz), 4.55 (d, 1H, J = 9.3 Hz), 4.10 (s, 1H), 3.11 (d, 1H, J = 9.3 Hz), the proton signals attributable to the alkyl side chain (C_8H_{17}) were not identifiable. MALDI-TOF MS calculated for $C_{110}H_{27}La_2N_5$ ([M]$^-$): 1695.04, found: 1695.38 m/z.

dx.doi.org/10.1021/ja307341g | J. Am. Chem. Soc. 2012, 134, 19401−19408

*6,6-La$_2$@C$_{80}$CH$_2$NOctCH-TCAQ (**2b**).* MALDI-TOF MS calculated for $C_{110}H_{27}La_2N_5$ ($[M]^-$): 1695.04, found: 1695.41 *m*/*z*. UV−vis−near-IR (toluene) λ_{max} 695 nm.

*Synthesis of 5,6-La$_2$@C$_{80}$CH$_2$NEtCH-Ph (**4**).* **4** was prepared according to previously reported synthetic procedures,[15] and was identified using the spectroscopic data thereof.

Theoretical Calculations. Geometries were optimized using the Gaussian 09 program[26] with the M06-2X[27] functionals. The basis set with relativistic effective core potential suggested by Hay and Wadt[28] was used for the La atom. The split valence 6-31G(d)[29] basis set was used for C, H, and N.

■ ASSOCIATED CONTENT

Supporting Information

Spectral data of **1a**, **2a** and **2b**, Cartesian coordinates of the optimized structures of **1**. This material is available free of charge via the Internet at http://pubs.acs.org.

■ AUTHOR INFORMATION

Corresponding Author

nazmar@quim.ucm.es; dirk.guldi@chemie.uni-erlangen.de; nagase@ims.ac.jp; akasaka@tara.tsukuba.ac.jp

Notes

The authors declare no competing financial interest.

■ ACKNOWLEDGMENTS

This work was supported in part by a Grant-in-Aid for Scientific Research on Innovative Areas (20108001, "π-Space"), a Grant-in-Aid for Scientific Research (A) (20245006) and (B) (24350019), The Next Generation Super Computing Project (Nanoscience Project), the Nanotechnology Support Project, Grants-in-Aid for Scientific Research on Priority Area (20036008 and 20038007), and a Specially Promoted Research from the Ministry of Education, Culture, Sports, Science, and Technology of Japan and The Strategic Japanese-Spanish Cooperative Program funded by JST and MINECO (Projects PLE-2009-0039 and PIB2010JP-00196). This work was also supported in part by the Deutsche Forschungsgemeinschaft Cluster of Excellence "Engineering of Advanced Materials", FCI, the Office of Basic Energy Sciences of the U.S. Department of Energy. Financial support was also provided by the MINECO of Spain (Projects CTQ2011-24652, PIB2010JP-00196, and Consolider-Ingenio 2010C-07-25200), CAM (MADRISOLAR Project P-PPQ-000225-0505).

■ REFERENCES

(1) Grätzel, M. *Acc. Chem. Res.* **2009**, *42*, 1788.

(2) For some recent reviews on organic photovoltaics, see: (a) Dennler, G.; Scharber, M. C.; Brabec, Ch. J. *Adv. Mater.* **2009**, *21*, 1323. (b) Kippelen, B.; Brédas, J.-J. *Energy Environ. Sci.* **2009**, *2*, 251. (c) Thompson, B. C.; Fréchet, J. M. J. *Angew. Chem., Int. Ed.* **2008**, *47*, 58. (d) Gunes, S.; Neugebauer, H.; Sariciftci, N. S. *Chem. Rev.* **2007**, *107*, 1324. (e) Imahori, H.; Umeyama, T. *J. Phys. Chem. C* **2009**, *113*, 9029. (f) Delgado, J. L.; Bouit, P.-A.; Filippone, S.; Herranz, M. A.; Martín, N. *Chem. Commun.* **2010**, *46*, 4853. (g) *Energy Environ. Sci.* **2011**, *4*, 2339, special issue on *Biomimetic Approaches to Artificial Photosynthesis*.

(3) Gust, D.; Moore, T. A.; Moore, A. L. *Acc. Chem. Res.* **2009**, *42*, 1890.

(4) (a) *Fullerenes*; Hirsch, A., Brettreich, M., Eds., Wiley-VCH: Weinheim, 2004. (b) *Carbon Nanotubes and Related Structures*; Guldi, D. M., Martín, N., Eds.; Wiley-VCH: Weinheim, 2010.

(5) (a) Liang, Y.; Xu, Z.; Xia, J.; Tsai, S.-T.; Wu, Y.; Li, G.; Ray, C.; Yu, L. *Adv. Mater.* **2010**, *22*, E135. (b) Huo, L.; Zhang, S.; Guo, X.; Xu, F.; Li, Y.; Hou, J. *Angew. Chem., Int. Ed.* **2011**, *50*, 9697.

(6) (a) *Chemistry of Nanocarbons*; Akasaka, T., Wudl, F., Nagase, S., Eds.; Wiley: Chichester, 2010. (b) Rudolf, M.; Wolfrum, S.; Guldi, D. M.; Feng, L.; Tsuchiya, T.; Akasaka, T.; Echegoyen, L. *Chem.—Eur. J.* **2012**, *18*, 5136.

(7) Ross, R. B.; Cardona, C. M.; Guldi, D. M.; Sankaranarayanan, S. G.; Reese, M. O.; Kopidakis, N.; Peet, J.; Walker, B.; Bazan, G. C.; Van Keuren, E.; Holloway, B. C.; Drees, M. *Nat. Mater.* **2009**, *8*, 208.

(8) Sato, S.; Seki, S.; Honsho, Y.; Wang, L.; Nikawa, H.; Luo, G.-F.; Lu, J.; Haranaka, M.; Tsuchiya, T.; Nagase, S.; Akasaka, T. *J. Am. Chem. Soc.* **2011**, *133*, 2766.

(9) Feng, L.; Rudolf, M.; Wolfrum, S.; Troeger, A.; Slanina, Z.; Akasaka, T.; Nagase, S.; Martín, N.; Ameri, T.; Brabec, C. J.; Guldi, D. M. *J. Am. Chem. Soc.* **2012**, *134*, 12190.

(10) Iiduka, Y.; Ikenaga, O.; Sakuraba, A.; Wakahara, T.; Tsuchiya, T.; Maeda, Y.; Nakahodo, T.; Akasaka, T.; Kako, M.; Mizorogi, N.; Nagase, S. *J. Am. Chem. Soc.* **2005**, *127*, 9956.

(11) Cai, T.; Xu, L.; Anderson, M. R.; Ge, Z.; Zuo, T.; Wang., X.; Olmstead, M. M.; Balch, A. L.; Gilbson, H. W.; Dorn, H. C. *J. Am. Chem. Soc.* **2006**, *128*, 8581.

(12) Guldi, D. M.; Feng, L.; Radhakrishnan, S. G.; Nikawa, H.; Yamada, M.; Mizorogi, N.; Tsuchiya, T.; Akasaka, T.; Nagase, S.; Herranz, A.; Martín, N. *J. Am. Chem. Soc.* **2010**, *132*, 9078.

(13) Ohkubo, K.; Ortiz, J.; Marín-Gomis, L.; Fernández-Lázaro, F.; Sastre-Santos, Á.; Fukuzumi, S. *Chem. Commun.* **2007**, 589.

(14) (a) Seoane, C.; Martín, N. In *Handbook of Organic Conductive Molecules and Polymers*, 4th ed.; Nalwa, H. S., Ed., Wiley: New York, 1997; Chapter 1, Vol. *1*. (b) Gómez, R.; Seoane, C.; Segura, J. L. *Chem. Soc. Rev.* **2007**, *36*, 1305.

(15) (a) Martín, N.; Hanack, M. *J. Chem. Soc., Chem. Commun.* **1988**, 1522. (b) Martín, N.; Behnisch, R.; Hanack, M. *J. Org. Chem.* **1989**, *54*, 2563. (c) Kini, A. M.; Cowan, D. O.; Gerson, F.; Möckel, R. *J. Am. Chem. Soc.* **1985**, *107*, 556. (d) Aumüller, A.; Hünig, S. *Liebigs Ann. Chem* **1984**, 618.

(16) (a) Maggini, M.; Scorrano, G.; Prato, M. *J. Am. Chem. Soc.* **1993**, *115*, 9798. (b) Prato, M.; Maggini, M. *Acc. Chem. Res.* **1998**, *31*, 519.

(17) Takano, Y.; Herranz, M. A.; Martín, N.; Radhakrishnan, S. G.; Guldi, D. M.; Tsuchiya, T.; Nagase, S.; Akasaka, T. *J. Am. Chem. Soc.* **2010**, *132*, 8048.

(18) (a) Braida, B.; Walter, C.; Engels, B.; Hiberty, P. C. *J. Am. Chem. Soc.* **2010**, *132*, 7631. (b) Ess, D. H.; Houk, K. N. T. *J. Am. Chem. Soc.* **2007**, *129*, 10646.

(19) (a) Yamada, M.; Okamura, M.; Sato, S.; Someya, I. C.; Mizorogi, N.; Tsuchiya, T.; Akasaka, T.; Kato, T.; Nagase, S. *Chem.—Eur. J.* **2009**, *15*, 10533. (b) Yamada, M.; Wakahara, T.; Nakahodo, T.; Tsuchiya, T.; Maeda, Y.; Akasaka, T.; Yoza, K.; Horn, E.; Mizorogi, N.; Nagase, S. *J. Am. Chem. Soc.* **2006**, *128*, 1402.

(20) ^{13}C NMR measurements of **1a** and **2a** were not obtained because of their low solubility. In both cases, precipitation was observed after several hours of ultrasonication of the solutions, even in good solvents for fullerenes such as CS_2 or ODCB.

(21) Illescas, M. B.; Martín, N. *J. Org. Chem.* **2000**, *65*, 5986.

(22) Maroto, E. E.; de Cozar, A.; Filippone, S.; Martin-Domenech, A.; Suarez, M.; Cossio, F. P.; Martín, N. *Angew. Chem., Int. Ed.* **2011**, *50*, 6060.

(23) Rodríguez-Fortea, A.; Campanera, J. M.; Cardona, C. M.; Echegoyen, L.; Poblet, J. M. *Angew. Chem., Int. Ed.* **2006**, *45*, 8176.

(24) Chaur, M. N.; Melin, F.; Ortiz, A. L.; Echegoyen, L. *Angew. Chem., Int. Ed.* **2009**, *48*, 7514.

(25) Santos, J.; Illescas; Martín, N.; Adrio, J.; Carretero, J. C.; Viruela, R.; Ortí, E.; Spänig, F.; Guldi, D. M. *Chem.—Eur. J.* **2011**, *17*, 2957.

(26) Frisch, M. J.; Trucks, G. W.; Schlegel, H. B.; Scuseria, G. E.; Robb, M. A.; Cheeseman, J. R.; Scalmani, G.; Barone, V.; Mennucci, B.; Petersson, G. A.; Nakatsuji, H.; Caricato, M.; Li, X.; Hratchian, H. P.; Izmaylov, A. F.; Bloino, J.; Zheng, G.; Sonnenberg, J. L.; Hada, M.; Ehara, M.; Toyota, K.; Fukuda, R.; Hasegawa, J.; Ishida, M.; Nakajima, T.; Honda, Y.; Kitao, O.; Nakai, H.; Vreven, T.; Montgomery, J. A., Jr.;

Peralta, J. E.; Ogliaro, F.; Bearpark, M.; Heyd, J. J.; Brothers, E.; Kudin, K. N.; Staroverov, V. N.; Kobayashi, R.; Normand, J.; Raghavachari, K.; Rendell, A.; Burant, J. C.; Iyengar, S. S.; Tomasi, J.; Cossi, M.; Rega, N.; Millam, J. M.; Klene, M.; Knox, J. E.; Cross, J. B.; Bakken, V.; Adamo, C.; Jaramillo, J.; Gomperts, R.; Stratmann, R. E.; Yazyev, O.; Austin, A. J.; Cammi, R.; Pomelli, C. J.; Ochterski, W.; Martin, R. L.; Morokuma, K.; Zakrzewski, V. G.; Voth, G. A.; Salvador, P.; Dannenberg, J. J.; Dapprich, S.; Daniels, A. D.; Farkas, O.; Foresman, J. B.; Ortiz, J. V.; Cioslowski, J. Fox, D. J. *Gaussian 09*, Revision A.02; Gaussian, Inc.: Wallingford, CT, 2009.

(27) Zhao, Y.; Truhlar, D. G. *Theory Chem. Acc.* **2008**, *120*, 215.

(28) Hay, P. J.; Wadt, W. R. *J. Chem. Phys.* **1985**, *82*, 299.

(29) (a) Ditchfield, R.; Hehre, W. J.; Pople, J. A. *J. Chem. Phys.* **1971**, *54*, 724. (b) Hehre, W. J.; Ditchfield, R.; Pople, J. A. *J. Chem. Phys.* **1972**, *56*, 2257.